

EFFECT OF ALKALI-TREATMENT ON TENSILE PROPERTIES OF KENAF LONG FIBERS

Y. Nitta^{1*}, J. Noda², K. Goda² and W-I. Lee³

¹ Graduate School of Science and Engineering, Yamaguchi University, Ube, Japan,

² Department of Mechanical Engineering, Yamaguchi University, Ube, Japan,

³ Department of Mechanical and Aerospace Engineering, Seoul National University, Seoul, Korea

*Corresponding author (p037ve@yamaguchi-u.ac.jp)

Keywords: *Alkali treatment, Kenaf fiber, Tensile strength, Fracture strain, X-ray diffraction*

1 Introduction

Recently, global environmental problems about CO₂ emission become serious concerns. Thus, a number of biomass-based material researches are nowadays being developed. Green composite using kenaf fiber and polylactic acid (PLA) is the promising material in the field of composite materials. It has already been used in cellular phones and car interior parts. However, practical kenaf/PLA composites are often produced as an injection molded material, while it has not been enough reported about the mechanical properties of long fiber reinforcement. On the other hand, some chemical treatments are applied to natural fibers to improve the interfacial properties between natural fibers and resin. Alkaline treatment is one of the most typical chemical treatments. Kawahara, et al. [1] explored the mechanical properties of alkali-treated kenaf fiber by changing concentration of the aqueous solution of NaOH in the relatively low range, i.e. 1 to 7 %. The results showed that tensile strength of the treated fibers did not change so largely. On the contrary, alkali-treated kenaf fiber reinforced composites indicated high flexural strength and modulus [2]. It is guessed from the above that, although low concentration alkali-treated kenaf fibers can improve mechanical properties of the composites, this is mainly caused by interfacial improvement. When single-cell type natural fibers such as ramie are mercerized by high concentration alkali solution, the mechanical properties are dramatically changed, especially in fracture strain[3]. On the other hand, the effect of mercerization has not been explored sufficiently for multi-cell type natural fibers such as kenaf.

The purpose of this study is thus to investigate the effect of high concentration alkali treatment on the tensile properties of kenaf fibers, which posses a relatively high content in lignin, inherent in multi-

cell type natural fibers. In addition, a new cross-sectional area measurement for alkali-treated kenaf fibers is proposed using a laser system.

2 Experimental

2.1 Materials

Kenaf fibers (*Hibiscus cannabinus*), harvested in Vietnam was used in this study. Alkali treatment was applied to the fibers in a 10wt%NaOH solution for two hours at room temperature or a 15wt%NaOH for one, two, four or six hours. Hereinafter, untreated fibers are denoted as UT, and alkali-treated fibers are denoted as “A” followed by (concentration) - (treating time). For example, A15-2 means alkali-treated fibers in a 15wt%NaOH solution for two hours.

2.2 Cross-sectional area measurement

In general, there are large variation in cross-sectional area of natural fibers. Although cross-section of kenaf fibers is a complicated shape, cross-sectional area of general natural fibers as well as kenaf has often been evaluated as a circular shape by measurement of fiber projection width. Circular shape assumption gives a large difference from actual cross-sectional area, and results in bringing over- or under- estimation in strength. Cross-sectional area of kenaf fibers was evaluated using the data-base approximation method (hereinafter, it is denoted as DBA) [4]. DBA method is based on the database for a distribution of actual fiber cross-sectional area obtained from cross-sectional pictorial images of natural fibers. As mentioned above, usually the fiber cross-sectional area is calculated assuming a projection width as a diameter, which is measured by optical microscope or laser system. Fig.1 shows a microphotograph of the cross-section of a kenaf fiber. As observed in the figure, the shape of the fiber cross-section is not circle. Actual fiber cross-sectional area of kenaf fibers, as indicated in

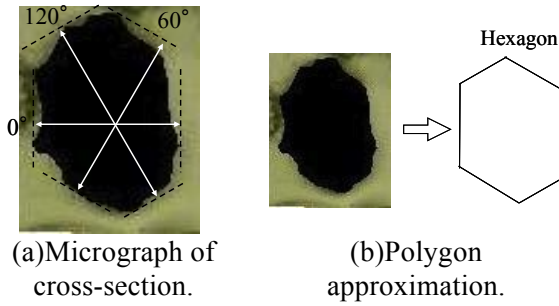
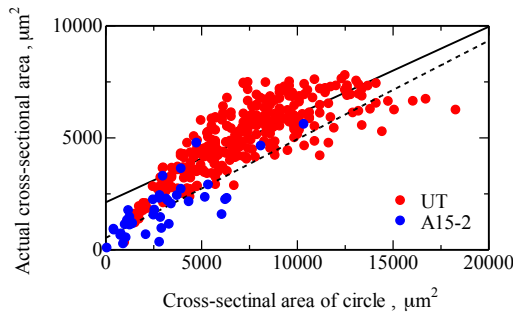
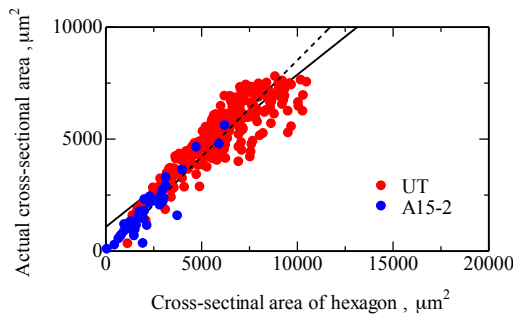


Fig.1. Optical micrograph of cross-section on a kenaf and polygon approximation.



(a) Circle-assumption



(b) Hexagon-assumption

Fig.2. Relationship of actual cross-sectional area with (a) circle-assumption area, and (b) hexagon-assumption area for kenaf fibers.

Painted area in black, were measured through an image analysis. At each image, the projective widths from three directions of 0, 60 and 120 degrees were measured as shown in Fig. 1. In this case, the cross-sectional area of the fiber was evaluated by assuming the shape of hexagon, composed of 3 diagonal lines corresponding to 3 projective widths. The relations between the actual cross-sectional area, and the circle and hexagon-assumed areas for kenaf 2(a) and (b) in red point, respectively. It is proved that correlation of the hexagon assumption area to

Table 1 Comparison of actual cross-sectional area with circle- and hexagon-assumption.

	Actual	Assumption	
		Circle	Hexagon
$A_c [\mu m^2]$	5010	7356	5783
CC	—	0.800	0.900

A_c : Cross-sectional area, CC: Coefficient of correlation.

the actual cross-sectional area is stronger than that of the circle-assumption area. Table 1 shows comparison of actual cross-sectional area with circle- and hexagon- assumption. From this table, it is found that more exact cross-section area of natural fibers can be evaluated through hexagon-assumption areas because the coefficients of correlation is higher. More appropriate approximation shape of cross-section area was examined by selecting a circle, ellipse, hexagon, pntagon, dodecagon or icositetragon. Correlation coefficient of each shape is shown in Fig. 3. Correlation coefficients after hexagon are around 0.9 and almost constant. Therefore, the fiber cross-sectional area calculated from the hexagon assumption in the above is valid. Hexagonal approximation equation obtained here was $y=0.68x+1080$. Fiber cross-sectional area was evaluated using this equation. Tensile strength calculated from hexagonal approximation is shown in the Table 2. It is considered that the corrected strength are close to exact values because their cross-sectional areas are based on the DBA.

2.3 Tensile test

Single fiber tensile tests were carried out using a tension and compression testing machine with a fine load cell. The gauge length of the tensile specimen was 25 mm, the tensile speed was 1.0 mm/min and the number of samples in each condition was ten. The projective width of these natural fibers were measured from three directions of 0, 60 and 120 degrees at 0.1 mm interval along their axial direction, using a laser scan micro-meter (LSM-500S, Mitutoyo Corporation). In this experiment the shape of cross-section is assumed as an hexagon. Displacement was measured using a laser displacement meter (KEYENCE, LS-7500).

3 Results and Discussion

3.1 Tensile properties

Experimental results are shown in Table 3. Tensile

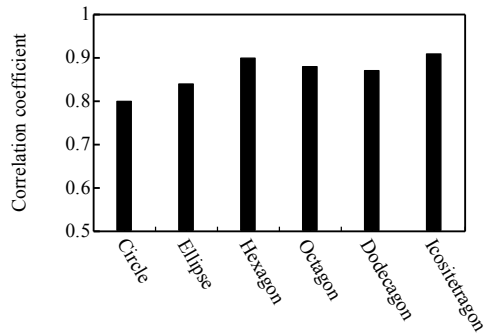


Fig.3. Correlation coefficients of assumed various shapes.

Table 2 Cross-sectional area and tensile strength calculated from hexagon-assumption cross-sections.

	Cross-sectional area [μm^2]	Tensile strength [MPa]
Measurement	4517	260
Approximation	3734	320

strength of A10 and A15 fibers decreased as compared to that of UT fibers. A15 fibers decrease in tensile strength with treating time. Young's modulus of A15 fibers was also largely lowered, one fifth to one fifteenth less than that of UT fibers. The degree of the decrease in modulus is larger as compared to the reference [3]. Alkali-treated kenaf fibers indicated at least about one- sixth of original Young's modulus as the NaOH concentration increases. On the other hand, the fracture strain increased, in the same manner as single-cell type natural fibers such as ramie. Especially A15-1 fibers show the largest fracture strain of all samples. From the viewpoint of toughness improvement, A15-1 fibers exhibit three times higher in fracture energy than UT fibers. Fig. 4 indicates typical stress-strain curves of untreated and alkali-treated kenaf fibers. Through the alkali treatment, the fibers decrease in strength and stiffness, as mentioned above. Especially, A15-4 and A15-6 fibers show a milder behavior in its slope at the initial stage, as compared to other fibers. It is guessed that lignin existing between cells was almost removed through the long time alkali treatments. According to SEM observation, A15-4 and A15-6 fibers lost their substance between cells, and looked like a fiber bundle. Therefore, it is estimated that the initial mild behavior is brought from unbalanced stress

Table 3 Tensile properties of untreated and alkali treated kenaf fibers.

Fiber Type	Number of samples	Tensile strength [MPa]	Young's modulus [GPa]	Fracture strain [%]
UT	10	320	30.8	1.28
A10-2	10	235	7.77	2.64
A15-1	10	263	6.67	6.14
A15-2	10	204	5.12	4.94
A15-4	10	198	5.21	3.57
A15-6	10	155	2.01	5.15

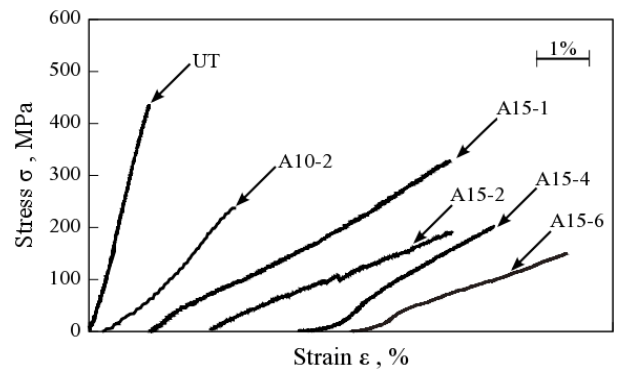


Fig.4. Typical stress-strain curves of kenaf fibers.

distribution in the separated cells.

3.2 X-ray diffraction approach

High concentration alkali treatment for natural fibers metamorphoses their crystalline structure from cellulose I to II, called mercerization [5]. Mercerized single-cell type natural fibers decrease in strength and stiffness, because of decrease in crystallinity index and occurrence of cellulose II, while the fibers are improved in toughness because of partial disappearance in binder (hemicellulose) [5]. In addition kenaf fibers treated in this study caused cell separation during alkali treatment, as mentioned above. Thus, X-ray diffraction analyses of alkali-treated kenaf fibers were carried out to identify the fiber structure.

Fig. 5 shows X-ray relative intensity of untreated and alkali-treated kenaf fibers. The results show that the peak of intensity of UT fibers exist at the diffraction angle $2\theta=16.5^\circ$ and 22.5° , and also A5 and A10 fibers show the peak at the same diffraction angles. The peak diffraction angles of A15 fibers starts to change to around 21.8° and 12.1° , the peak

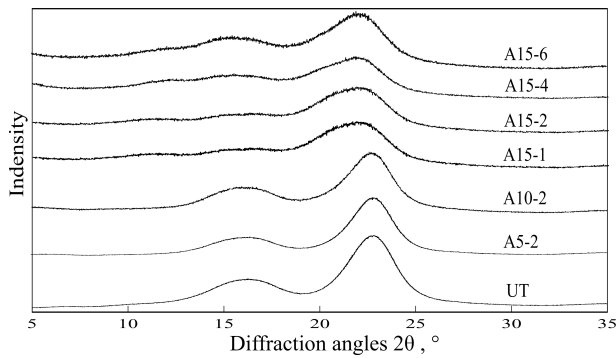


Fig.5. X-ray diffraction diagrams of untreated and alkali-treated kenaf fibers.

angles of cellulose II. However the previous peak, $2\theta=16.5^\circ$, still remains in the diagram as shown in Fig.5. This means that, although it is not perfectly done under the given conditions, mercerization occurs partly in alkali-treated multi-cell type fibers.

Fig. 6 shows the crystallinity index of alkali-treated kenaf fibers. A5 and A10 fibers indicate roughly the same values as UT fibers. On the other hand, the crystallinity index of A15 fibers decreased about 25% less than that of UT fibers. In the case of ramie fibers, also the crystallinity index decreased from 70% - 80% levels to approximately 50% [4]. Such decrease in crystallinity index as well as partial mercerization cause the decrease in strength and stiffness of multi-cell type natural fibers, similarly to single-cell type ones. However, the degree of the decrease in Young's modulus is quite serious as mentioned above. Thus, we consider, resin infiltration to inter-cells would be a key-point in developing kenaf long fiber green composites.

Fig. 7 shows the crystalline transition rate of alkali-treated kenaf fibers. Concentration of 5 wt% as compared to untreated fiber did not change

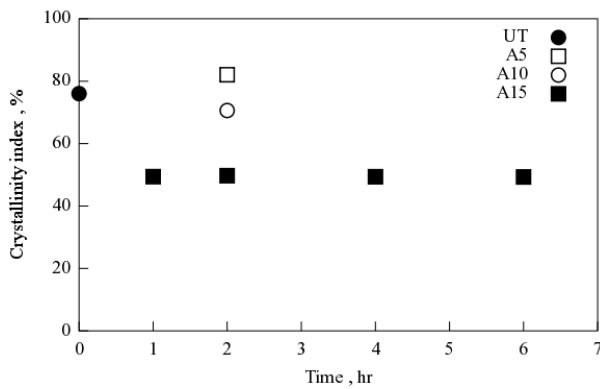


Fig.6. Effect of NaOH concentration on the crystallinity index of kenaf fibers.

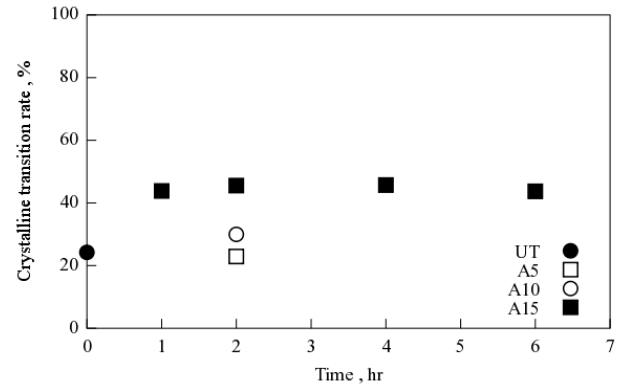


Fig.7. Effect of NaOH concentration on the crystalline transition rate of kenaf fibers.

crystalline structure. Crystalline transition rate increase from concentration of 10 wt%. Moreover, crystalline transition rate of concentration of 15 wt% has increased to about 45%. However, alkali-treated kenaf fiber in the concentration of 15 wt% did not completely bring mercerization.

3.3 DBA for alkali-treated kenaf fiber

Cross-sectional shape of kenaf fiber was drastically changed by high concentration alkali treatment, as shown in Fig. 8(a). Many gaps between cells occurred due to removal of lignin. Thus, alkali-treated kenaf fibers should be reconsidered in evaluating cross-sectional area. In this study, DBA for alkali-treated fiber is newly proposed as follows:

1. Cross-sectional area of each cell is approximated as an ellipse as shown in Fig. 8(b), and summed up. This is evaluated as actual cross-sectional area.
2. Cross-sectional area of each polygon shape obtained from projection widths is estimated similarly to the conventional DBA.
3. Assumed cross-sectional area obtained in 2 is corresponded to actual cross-sectional area, and approximation equation is derived.

Alkali treatment condition used here was 15 wt% and 2 hours. The relations between the actual cross-sectional area and the circle- and hexagon-assumed areas for alkali-treated kenaf fiber are added to Fig. 2 by blue points, respectively. The added blue points are located slightly under the original red points, in untreated fibers is replaced to void area. It is proved that the correlation coefficient of hexagon-assumption area to actual cross-sectional area is higher than that of circle-assumption area. Table 4

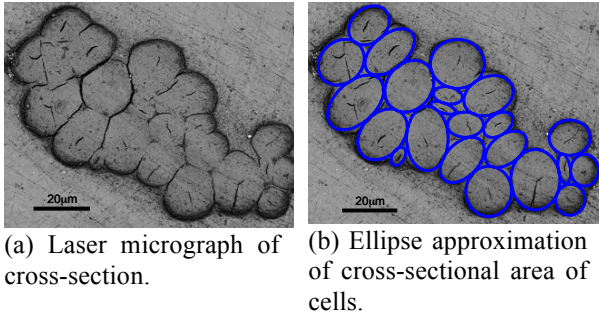


Fig.8. Laser micrograph of cross-section on a alkali-treated kenaf fiber.

shows comparison of actual cross-sectional area with circle- and hexagon- assumption for alkali-treated fibers. Hexagonal approximation obtained was $y=0.86x-84$. This evaluation method is denoted as DBA-AT. DBA-AT was used here for hexagonal approximation. The tensile test results corrected by DBA-AT are shown in Table 5. Cross-sectional area corrected by DBA-AT is smaller than that by the assumed area, and results in increasing the tensile properties of the alkali-treated fibers. DBA-AT was corrected in cross-sectional area about 20% smaller. The intercept in linear approximation of DBA-AT starts from near zero as shown in Fig. 2. In addition, mechanical properties are largely improved through DBA-AT. However, actual cross-sectional area of this calculation method is underestimated because gaps are exaggeratedly evaluated at the process of image analysis. Actual tensile strength may be placed between DBA and DBA-AT approximation values.

4 Conclusion

Tensile tests of alkali-treated kenaf fibers were carried out. Moreover, crystallinity index and crystalline transition rate of the kenaf fiber were obtained from X-ray diffraction analysis. And the DBA for alkali-treated fibers was newly proposed.

Table 4 Correlation of actual cross-sectional area of alkali-treated fiber with circle- and hexagon-assumption.

	Actual	Assumption	
		Circle	Hexagon
$A_c [\mu m^2]$	1875	3037	2277
CC	—	0.795	0.933

Table 5 Cross-sectional area and tensile properties corrected from DBA-AT.

Fiber type	A_c [μm^2]	A_c^* [μm^2]	σ_f [MPa]	σ_f^* [MPa]	E [GPa]	E* [GPa]
UT	4517	-	260	-	25.8	-
A10-2	3773	2325	214	282	6.21	9.34
A15-1	2805	2510	303	354	7.67	9.00
A15-2	2843	2377	190	227	4.63	5.53
A15-4	2400	2025	255	303	6.67	7.65
A15-6	3426	2862	156	187	2.02	2.54

σ_f : Tensile strength, E: Young's modulus, * means corrected value.

As a result:

1. Fracture strain increases and tensile strength decreases when subjected to high concentration alkali-treated fiber.
2. Crystallinity index decrease as the concentration of alkali treatment increases. Moreover, crystalline transition rate increase as the concentration of alkali treatment increases. In the case of 15wt%, crystallinity index and crystalline transition rate were independent of treatment times.
3. DBA-AT can be a lower limit for evaluation of actual cross-sectional area of the alkali-treated fibers.

References

- [1] Y. Kawahara, K. Tadokoro, R. Endo, M. Shioya, Y. Sugimura and T. Furusawa, *SEN'I GAKKAISHI*, Vol. 61, pp115, 2005.
- [2] S.H. Aziz and M.P. Ansell, *Composites Science and Technology*, Vol. 64, pp1219, 2004.
- [3] K. Goda, M.S. Sreekala, A. Gomes, T. Kaji and J.. Ohgi, *Composite: Part A*, Vol 37, 2213-2220, 2006.
- [4] Y. Terasaki, J. Noda and K. Goda, *The 2nd International Conference on Multi-Functional Materials and Structures*, by CD, 2009.
- [5] K. Haraguchi, N. Suizu, T. Uno, K. Goda, J. Noda, and J. Ohgi, *Journal of The Society of Materials Science*, Vol. 58, pp 375-377, 2009.